Journal of Molecular Structure 965 (2010) 1–6

Contents lists available at ScienceDirect

Journal of Molecular Structure

journal homepage: www.elsevier.com/locate/molstruc

Synthesis, structural characterization, thermal and electrochemical studies of Mn(II), Co(II), Ni(II) and Cu(II) complexes containing thiazolylazo ligands

S.S. Chavan *, V.A. Sawant

Department of Chemistry, Shivaji University, Kolhapur (MS) 416 004, India

ARTICLE INFO

Article history:
Received 22 August 2009
Received in revised form 28 October 2009
Accepted 1 November 2009
Available online 6 November 2009

Keywords:
Azo complexes
ESR spectra
Thermal analysis
Electrochemistry

ABSTRACT

Some thiazolylazo derivatives and their metal complexes of the type $[M(L)(H_2O)Cl]$; M = Mn(II), Co(II), Ni(II), Cu(II) and L = 6-(2′-thiazolylazo)-2-mercapto-quinazolin-4-one (HL_1), 6-(4′-phenyl-2′-thiazolylazo)-2-mercapto-quinazolin-4-one (HL_2), 6-(2′-thiazolylazo)-2-mercapto-3-(*m*-tolyl)-quinazolin-4-one (HL_3) and 6-(4′-phenyl-2′-thiazolylazo)-2-mercapto-3-(*m*-tolyl)-quinazolin-4-one (HL_4) have been prepared. All the complexes were characterized on the basis of elemental analysis, molar conductance, magnetic moment, IR, UV–vis, ESR, TG-DTA and powder X-ray diffraction studies. IR spectra of these complexes reveal that the complex formation occurred through thiazole nitrogen, azo nitrogen, imino nitrogen and sulfur atom of the ligands. On the basis of electronic spectral data and magnetic susceptibility measurement octahedral geometry has been proposed for the Mn(II), Co(II) and Ni(II) complexes and distorted octahedral geometry for the Cu(II) complexes. Electrochemical behavior of Ni(II) complexes exhibit quasireversible oxidation corresponding to Ni(III)/Ni(II) couple along with ligand reduction. X-ray diffraction study is used to elucidate the crystal structure of the complexes.

1. Introduction

Arylazo compounds are interesting because they are involved in many biological reactions [1,2]; and in analytical chemistry as complexing agents for the determination of some metal ions, spectrophotometrically [3,4]. They are important in drugs and show a variety of interesting biological activities including antimicrobial activities [5–7], anti-inflammatory activities [8] and pesticidals activities [9]. Due to presence of the azo (—N=N—) group these compounds possess several distinctive properties including aggregation, optical data storage and tautomerism which define as a distinct class of dyestuffs [10,11]. Among various azo compounds thiazolylazo derivatives have attracted much attention as analytical reagents owing to their high sensitivity and selectivity [12,13]. They are used in chemical and analytical methods including spectrophotometry, solid phase extraction, liquid chromatography and electrochemistry [14]. The use of thiazolylazo derivatives in spectrophotometry is based on the coloured compounds resulting from their reaction with most of the transition metals. They can form different types of coordination compounds particularly with transition metals due to the several electron rich donor centers with unusual structural and chemical properties. Because of the importance of thiazolylazo derivatives and their ability to act as polyfunctional ligand many studies on their metal complexes have been carried out [15–18].

In this paper we report the synthesis of new thiazolylazo ligands 6-(2′-thiazolylazo)-2-mercapto-quinazolin-4-one (HL_1), 6-(4′-phenyl-2′-thiazolylazo)-2-mercapto-quinazolin-4-one (HL_2), 6-(2′-thiazolylazo)-2-mercapto-3-(*m*-tolyl)-quinazolin-4-one (HL_3) and 6-(4′-phenyl-2′-thiazolylazo)-2-mercapto-3-(*m*-tolyl)-quinazolin-4-one (HL_4) and their legation behavior with Mn(II), Co(II), Ni(II) and Cu(II). The complexes prepared were characterized on the basis of elemental analysis, conductance, magnetic moment, TG-DTA, X-ray crystallography and spectral (IR, UV–vis and ESR) studies. Electrochemical behavior of these complexes was discussed.

2. Experimental

2.1. Materials

All the chemicals used were pure and of analytical reagents grade. 4-Phenyl-2-aminothiazole [19], 2-mercapto-quinazolin-4-one [20] and 2-mercapto-3-(*m*-tolyl)-quinazolin-4-one [21] were synthesized by reported method. Solvents were purified and dried according to standard procedure.

2.2. Physical measurements

Microanalysis (C, H, N and S) were performed on a Thermo Finnigan FLASH EA-112 CHNS analyzer. Electronic spectra were re-

---

* Corresponding author. Tel.: +91 231 2609164; fax: +91 231 2691533.
E-mail address: sanjaycha2@rediffmail.com (S.S. Chavan).

0022-2860/$ - see front matter © 2009 Elsevier B.V. All rights reserved.
doi:10.1016/j.molstruc.2009.11.010

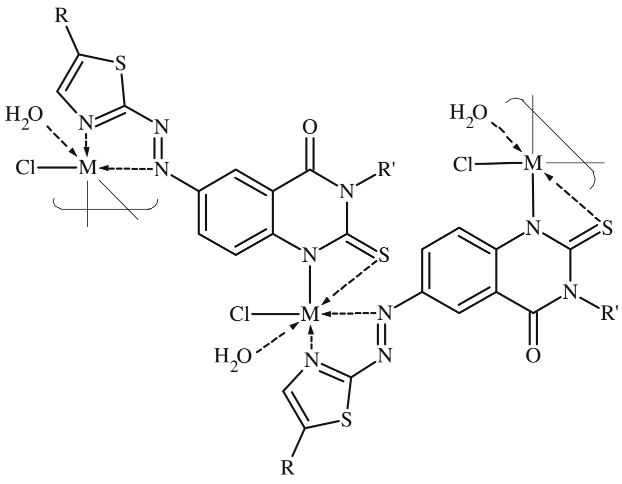

R = H, C_6H_5; R' = H, m-tolyl; M = Mn(II), Co(II), Ni(II) and Cu(II)

Fig. 1. Proposed structure for the metal complexes.

corded on a Shimadzu-3600 UV–vis-NIR spectrophotometer. Magnetic susceptibility was measured on Gouy balance at room temperature using a Johnson Matthey Alfa MKI magnetic susceptibility balance, with $Hg[Co(SCN)_4]$ as calibrant. Molar conductance (Λ_M) was measured on the ELICO (CM-185) conductivity bridge using ca. 10^{-3} M solution in DMF. Infrared spectra were recorded on Perkin-Elmer FT-IR-100 spectrometer as KBr pellets in the 4000–400 cm^{-1} spectral range. ESR spectra of the complexes were recorded at room temperature on Varian E-112 spectrometer using TCNE as the standard. Cyclic voltammetry measurements were performed with Electrochemical Quartz Crystal Microbalance CHI-400. A standard three electrode system, consisting of Pt disk working electrode, Pt wire counter electrode and Ag/AgCl reference electrode containing aqueous 3 M KCl were used. X-ray powder analysis were carried out by using Philips PW 3710 diffractometer operated at 40 kV and 30 mA generator using CuKα line at 1.54056 Å as the radiation source.

2.3. Synthesis of HL_{1-4} ligands (diazotization and coupling)

The ligands 6-(2′-thiazolylazo)-2-mercapto-quinazolin-4-one (HL_1), 6-(4′-phenyl-2′-thiazolylazo)-2-mercapto-quinazolin-4-one (HL_2), 6-(2′-thiazolylazo)-2-mercapto-3-(*m*-tolyl)-quinazolin-4-one (HL_3) and 6-(4′-phenyl-2′-thiazolylazo)-2-mercapto-3-(*m*-tolyl)-quinazolin-4-one (HL_4) were synthesized by diazotization of substituted 2-aminothiazole using H_2SO_4 and $NaNO_2$ according to a procedure analogous to that described earlier [22]. The diazotized solution so formed was coupled with 2-mercapto-quinazolin-4-one (0.178 g, 1 mmol) or 2-mercapto-3-(*m*-tolyl)-quinazolin-4-one (0.268 g, 1 mmol) in 30 mL of ethanol below 5 °C. The product formed was collected by filtration, washed well with water and recrystalized from ethanol.

2.4. Preparation of metal complexes (Fig. 1)

The complexes of Mn(II), Co(II), Ni(II) and Cu(II) were prepared by mixing ethanolic solution (5 mL) of the organic ligand (1 mmol, 0.289 g, HL_1, 0.365 g, HL_2, 0.379 g, HL_3, 0.455 g, HL_4) with solution (5 mL) of appropriate metal chloride (1 mmol, 0.197 g, $MnCl_2.4H_2O$, 0.237 g, $CoCl_2{\cdot}6H_2O$, 0.237 g, $NiCl_2{\cdot}6H_2O$ and 0.170 g, $CuCl_2{\cdot}2H_2O$) in ethanol. The resultant mixture was refluxed for 2 h on a water bath and the solid complex precipitated was collected by filtration, washed several times with 1:1 ethanol:water mixture and dried under vacuum over $CaCl_2$ at room temperature .

3. Results and discussion

The results of the elemental analysis of ligands HL_{1-4} and their Mn(II), Co(II), Ni(II) and Cu(II) complexes are recorded in Table 1. All the metal complexes are coloured, non-hygroscopic and are fairly stable at room temperature. They are found to be insoluble in common organic solvents like methanol, ethanol, dichloromethane, acetonitrile except DMF and DMSO. The molar conductance data (Table 1) of the complexes in DMF at 10^{-3} M is in the range 13–36 Ω^{-1} cm^2 mol^{-1}, which indicates nonelectrolytic nature of the complexes suggesting that the Cl^- anion is coordinated to metal ion. This is further supported by proposed general formulae of the complexes as suggested depending upon the results of elemental analysis and IR spectra.

3.1. IR spectral studies

The main stretching frequencies of the IR spectra of ligands (HL_{1-4}) and their complexes are listed in Table 2. The IR spectra

Table 1
Analytical and physico-chemical data of the ligands and their metal complexes.

Complex	M. F. (colour)	Yield	M.P. (°C)	Analytical data % found (calculated)					Λ_M (Ω^{-1} cm^2 mol^{-1})
				M	C	H	N	S	
HL_1	$C_{11}H_7N_5OS_2$ (brown)	73	148		45.30 (45.66)	2.28 (2.44)	24.35 (24.20)	21.98 (22.16)	
$[Mn(L_1)(H_2O)Cl]$	$C_{11}H_8N_5O_2S_2ClMn$ (yellow brown)	64	>300	13.72 (13.85)	33.12 (33.30)	1.89 (2.03)	17.81 (17.65)	16.02 (16.16)	36
$[Co(L_1)(H_2O)Cl]$	$C_{11}H_8N_5O_2S_2ClCo$ (brown)	65	>300	14.68 (14.71)	32.76 (32.97)	2.13 (2.01)	17.52 (17.48)	15.83 (16.00)	30
$[Ni(L_1)(H_2O)Cl]$	$C_{11}H_8N_5O_2S_2ClNi$ (pale brown)	70	>300	14.36 (14.66)	32.84 (32.99)	1.94 (2.01)	17.59 (17.49)	16.08 (16.01)	15
$[Cu(L_1) (H_2O)Cl$	$C_{11}H_8N_5O_2S_2ClCu$ (dark brown)	66	>300	15.53 (15.68)	32.46 (32.59)	1.79 (1.99)	17.04 (17.28)	15.96 (15.82)	34
HL_2	$C_{17}H_{11}N_5OS_2$ (violet)	69	154		55.59 (55.87)	2.89 (3.03)	19.32 (19.16)	17.38 (17.55)	
$[Mn(L_2)(H_2O)Cl]$	$C_{17}H_{12}N_5O_2S_2ClMn$ (brown)	70	>300	11.52 (11.62)	43.12 (43.18)	2.47 (2.56)	14.97 (14.81)	13.44 (13.56)	29
$[Co(L_2)(H_2O)Cl]$	$C_{17}H_{12}N_5O_2S_2ClCo$ (brown)	65	>300	12.24 (12.36)	42.67 (42.82)	2.49 (2.54)	14.78 (14.69)	13.37 (13.45)	14
$[Ni(L_2)(H_2O)Cl]$	$C_{17}H_{12}N_5O_2S_2ClNi$ (pinkish violet)	66	>300	12.26 (12.32)	42.73 (42.84)	2.61 (2.54)	14.83 (14.69)	13.32 (13.46)	19
$[Cu(L_2)(H_2O)Cl]$	$C_{17}H_{12}N_5O_2S_2ClCu$ (dark brown)	68	>300	13.15 (13.20)	42.33 (42.41)	2.39 (2.51)	14.63 (14.55)	13.27 (13.32)	32
HL_3	$C_{18}H_{13}N_5OS_2$ (brown)	65	179		56.83 (56.97)	3.54 (3.45)	18.84 (18.46)	16.53 (16.90)	
$[Mn(L_3)(H_2O)Cl]$	$C_{18}H_{14}N_5O_2S_2ClMn$ (yellow brown)	70	>300	11.16 (11.28)	44.36 (44.41)	2.79 (2.90)	14.56 (14.38)	13.08 (13.17)	26
$[Co(L_3)(H_2O)Cl]$	$C_{18}H_{14}N_5O_2S_2ClCo$ (brown)	68	>300	11.97 (12.01)	44.13 (44.04)	2.92 (2.87)	14.36 (14.27)	12.93 (13.07)	30
$[Ni(L_3)(H_2O)Cl]$	$C_{18}H_{14}N_5O_2S_2ClNi$ (pinkish violet)	66	>300	11.85 (11.96)	43.87 (44.07)	2.78 (2.88)	14.51 (14.27)	13.12 (13.07)	20
$[Cu(L_3)(H_2O)Cl]$	$C_{18}H_{14}N_5O_2S_2ClCu$ (dark brown)	69	>300	12.73 (12.83)	43.51 (43.63)	2.69 (2.85)	14.29 (14.13)	13.04 (12.94)	18
HL_4	$C_{24}H_{17}N_5O_2S_2$ (violet)	76	186		63.07 (63.28)	3.69 (3.76)	15.43 (15.37)	13.94 (14.08)	
$[Mn(L_4)(H_2O)Cl]$	$C_{24}H_{18}N_5O_2S_2ClMn$ (light brown)	66	>300	9.62 (9.76)	51.13 (51.20)	3.18 (3.22)	12.66 (12.44)	11.27 (11.39)	22
$[Co(L_4)(H_2O)Cl]$	$C_{24}H_{18}N_5O_2S_2ClCo$ (brown)	71	>300	10.27 (10.39)	50.67 (50.84)	3.24 (3.20)	12.49 (12.35)	11.37 (11.31)	13
$[Ni(L_4)(H_2O)Cl]$	$C_{24}H_{18}N_5O_2S_2ClNi$ (pinkish violet)	68	>300	10.24 (10.36)	50.74 (50.87)	3.13 (3.20)	12.27 (12.36)	11.53 (11.32)	26
$[Cu(L_4)(H_2O)Cl]$	$C_{24}H_{18}N_5O_2S_2ClCu$ (dark brown)	70	>300	11.07 (11.12)	50.34 (50.43)	3.12 (3.17)	12.48 (12.25)	11.17 (11.22)	30

Table 2
Infrared spectral data of the ligands and metal complexes.

Compound	νH_2O	νNH	ν(C=N)	ν(N=N)	νC=O	Thioamide bands				ν M–N
						I	II	III	IV	
HL_1		3081	1624	1458	1686	1568	1307	978	870	
$[Mn(L_1)(H_2O)Cl]$	3445	3060	1610	1424	1690	1567, 1505	1299	978	857	461
$[Co(L_1)(H_2O)Cl]$	3460	3065	1618	1421	1689	1568, 1507	1300	978	865	459
$[Ni(L_1)(H_2O)Cl]$	3478	3060	1615	1415	1697	1560, 1507	1295	980	860	465
$[Cu(L_1)\ (H_2O)Cl$	3432	3056	1611	1418	1700	1549, 1505	1327	976	863	455
HL_2		3087	1620	1448	1685	1562	1327	977	874	
$[Mn(L_2)(H_2O)Cl]$	3436	3063	1613	1432	1690	1554, 1504	1313	977	857	469
$[Co(L_2)(H_2O)Cl]$	3440	3056	1609	1425	1700	1540, 1505	1319	979	860	459
$[Ni(L_2)(H_2O)Cl]$	3478	3059	1611	1428	1690	1558, 1504	1309	977	857	461
$[Cu(L_2)(H_2O)Cl]$	3421	3060	1608	1420	1697	1560, 1507	1295	980	863	460
HL_3		3245	1618	1445	1680	1533	1339	988	842	
$[Mn(L_3)(H_2O)Cl]$	3442	–	1593	1424	1686	1566, 1540	1316	989	835	465
$[Co(L_3)(H_2O)Cl]$	3435	–	1603	1415	1682	1560, 1538	1298	988	837	454
$[Ni(L_3)(H_2O)Cl]$	3447	–	1598	1420	1698	1579, 1540	1320	991	832	460
$[Cu(L_3)(H_2O)Cl]$	3436	–	1601	1412	1686	1566, 1541	1303	985	836	463
HL_4		3248	1624	1453	1687	1538	1342	990	848	
$[Mn(L_4)(H_2O)Cl]$	3460	–	1614	1438	1698	1573, 1540	1320	986	835	465
$[Co(L_4)(H_2O)Cl]$	3430	–	1609	1442	1702	1566, 1543	1316	990	837	458
$[Ni(L_4)(H_2O)Cl]$	3420	–	1603	1428	1695	1570, 1541	1320	991	832	470
$[Cu(L_4)(H_2O)Cl]$	3433	–	1597	1435	1700	1573, 1543	1305	987	837	459

Thioamide bands: Band-I (δNH + δC–N); Band-II (νC=N + δNH + δCH + νC=S); Band-III (νC = S + νC=N); Band-IV (νC=S).

of ligands and their complexes are found to be quite complex as they in general exhibit large number of bands of varying intensities. However, all the ligands $HL_{1\text{-}4}$ are capable of exhibiting thione–thiol tautomerism. In the IR spectra of ligands ($HL_{1\text{-}4}$), ν(NH) band appeared at 3081–3248 cm^{-1} and absence of ν(SH) band near 2600 cm^{-1} shows the thione structural form of the ligands in solid state. This ν(NH) band shifting to lower frequency (3056–3065 cm^{-1}) in the complexes of HL_1 and HL_2 and disappearing in the complexes of HL_3 and HL_4, provides strong evidence for involvement of ligand coordination in deprotonated form. This is also supported by the appearance of ν(M–N) band at 454–470 cm^{-1} in the complexes. The characteristic ν(C=O) frequency of ligands at 1680–1687 cm^{-1} remaining unaltered in all the complexes indicates the absence of bonding through carbonyl oxygen of the ligands [23]. The spectral region 1400–1630 cm^{-1} is quite complicated due to presence of ν(C=C), ν(C=N) and ν(N=N) stretching frequencies. A strong band observed at 1618–1624 cm^{-1} in the spectra of all ligands ($HL_{1\text{-}4}$) is due to ν(C=N) of thiazole nitrogen. This band shifted to lower frequencies in the complexes indicates involvement of thiazole nitrogen in coordination [24]. However, the band appearing at the frequency range 1445–1458 cm^{-1} in the spectra of ligands assigned to -N=N- group shifted to lower frequency (1412–1442 cm^{-1}) in the complexes indicates involvement of azo nitrogen in coordination with metal ion [25].

All the four ligands contain a thioamide group (H–N–C=S) and give rise to four characteristic bands (I, II, III and IV) at 1533–1579, 1307–1342, 976–990 and 842–870 cm^{-1} in their infrared spectra [23]. The thioamide band-I [δ(NH) + δ(C–N)] observed at ~1540 cm^{-1}, splits up in the spectra of the complexes also suggesting the coordination through imino nitrogen atom of the ligands. The two bands appearing at the frequency ~1340 cm^{-1} [ν(C=N) + δ(NH) + δ(CH) + ν(C=S)] thioamide band-II and ~845 cm^{-1} [ν(C=S)] thioamide band-IV in the spectra of ligands have been shifted to lower frequencies in the ranges 1292–1327 and 832–865 cm^{-1}, respectively, indicating coordination of thione/thiolato sulfur. The thioamide band-III observed at ~980 cm^{-1} in the ligands $HL_{1\text{-}4}$ reduces in intensity on coordination with metal ion [26]. In the spectra of all complexes a broad band observed at around 3440 cm^{-1} together with new band at around 826 cm^{-1} indicating the presence of water molecules in coordination sphere of the complexes [27].

3.2. Magnetic moments and electronic spectra

Magnetic moments and electronic spectra of the complexes are listed in Table 3. The absorption spectra of ligands $HL_{1\text{-}4}$ shows four absorption bands in the UV and visible region. The first two bands observed at 226–220 and 257–245 nm undoubtedly originate from the perturbed local excitation of the phenyl group. The bands located at 328–319 and 466–453 nm corresponds to the $\pi \rightarrow \pi^*$ and $n \rightarrow \pi^*$ transitions of the azo group [28]. However, the spectra of complexes shows bathochromic shift in comparison with free ligands.

The Mn(II) complexes exhibit three weak absorption bands at 720–714, 625–600 and 512–500 nm attributed to $^6A_{1g} \rightarrow {}^4T_{1g}$ (^4G), $^6A_{1g} \rightarrow {}^4T_{2g}$ (^4G) and $^6A_{1g} \rightarrow {}^4A_{1g}, {}^4E_g$ transitions, respectively. These are consistent with an octahedral geometry around Mn(II) ion in all complexes. The magnetic moment values of Mn(II) complexes in the range 5.71–5.83μ_B are an indicative of octahedral geometry [29].

Table 3
Magnetic moment and electronic spectral data of the complexes.

Compound	μ_{eff} (μ_B)	$\pi \rightarrow \pi^*$ and $n \rightarrow \pi^*$ transitions (nm) (λ_{max} in DMF)	d → d transitions (nm) (λ_{max} in DMF)
HL_1		220, 245, 319, 453	
$[Mn(L_1)(H_2O)Cl]$	5.73	262, 337, 408	505, 625, 714
$[Co(L_1)(H_2O)Cl]$	4.78	263, 348, 413	543, 655
$[Ni(L_1)(H_2O)Cl]$	2.92	253, 350, 421	535, 679, 956
$[Cu(L_1)\ (H_2O)Cl$	1.79	265, 340, 426	660
HL_2		223, 248, 320, 458	
$[Mn(L_2)(H_2O)Cl]$	5.71	260, 349, 410	500, 620, 720
$[Co(L_2)(H_2O)Cl]$	4.81	270, 335, 418	542, 650
$[Ni(L_2)(H_2O)Cl]$	3.02	267, 342, 414	536, 684, 957
$[Cu(L_2)(H_2O)Cl]$	1.78	267, 347, 420	659
HL_3		225, 254, 326, 463	
$[Mn(L_3)(H_2O)Cl]$	5.79	276, 360, 412	512, 624, 717
$[Co(L_3)(H_2O)Cl]$	4.93	270, 351, 414	542, 654
$[Ni(L_3)(H_2O)Cl]$	2.92	274, 362, 425	535, 687, 948
$[Cu(L_3)(H_2O)Cl]$	1.78	258, 365, 430	663
HL_4		226, 257, 328, 466	
$[Mn(L_4)(H_2O)Cl]$	5.83	264, 364, 408	510, 600, 719
$[Co(L_4)(H_2O)Cl]$	4.86	267, 360, 418	541, 649
$[Ni(L_4)(H_2O)Cl]$	2.89	274, 349, 420	538, 690, 961
$[Cu(L_4)(H_2O)Cl]$	1.76	272, 367, 427	667

The electronic spectra of Co(II) complexes shows two d–d transitions at 655–649 and 543–541 nm that may be assigned to $^4T_{1g}(^4F) \rightarrow {}^4A_{2g}(^4F)$ and $^4T_{1g}(^4F) \rightarrow {}^4T_{1g}(^4P)$ transitions, respectively. These transitions suggest an octahedral geometry around Co(II) ion [30]. The μ_{eff} value measured for the Co(II) complexes is in the range 4.78–4.93μ_B, which is fairly close to those reported for the three unpaired electrons of Co(II) ion in an octahedral environment [31].

The Ni(II) complexes exhibit three absorption bands at 961–948, 690–679 and 538–535 nm attributed to $^3A_{2g}(F) \rightarrow {}^3T_{2g}(F)$, $^3A_{2g}(F) \rightarrow {}^3T_{1g}(F)$ and $^3A_{2g}(F) \rightarrow {}^3T_{1g}(P)$ transitions, respectively. These results are compatible with the reported values for the octahedral Ni(II) complexes [32]. The room temperature magnetic moment values of Ni(II) complexes are 2.89–3.02μ_B which is in normal range observed for octahedral Ni(II) complexes [33].

The electronic spectra of Cu(II) complexes show a broad band centered at ~660 nm which could be attributed to $^2Eg \rightarrow {}^2T_{2g}$ transition characterized by Cu(II) ion in octahedral geometry [34]. The octahedral geometry of Cu(II) ion in all complexes is confirmed by the measured magnetic moment values in the 1.76–1.79μ_B range which is in harmony with the reported value.

3.3. Thermal studies

The thermal decomposition of Mn(II), Co(II), Ni(II) and Cu(II) complexes of the ligand HL_1 was studied using the TG-DTA in the temperature range 50–800 °C. In Mn(II) and Ni(II) complexes the first decomposition step occurs within the temperature range 148–282 °C with an accompanying DTA peak at 233 °C for Mn(II) and 258 °C for Ni(II) complex, estimated mass loss of 4.54% and 4.49%, respectively. The temperatures at which these losses are observed suggest the presence of one coordinated water molecule in the complexes. In Co(II) and Cu(II) complexes the first decomposition step occurs within the temperature range of 143–282 °C with an estimated mass loss of 4.49% and 4.44%, respectively. An accompanying DTA peak observed for Co(II) and Cu(II) at 240 and 238 °C, respectively, can be attributed to loss of one water molecule. Above 250 °C the complexes decompose in a gradual manner rather than with the sharp decomposition which may be due to fragmentation and thermal degradation of the organic moiety, as DTA curve shows exothermic peak. All these complexes show residue not confirming to the corresponding metal oxides even at 800 °C indicating that decomposition of organic moiety remains incomplete even at this temperature. The Fig. 2 is a representative example for thermal analysis of the metal complexes under study.

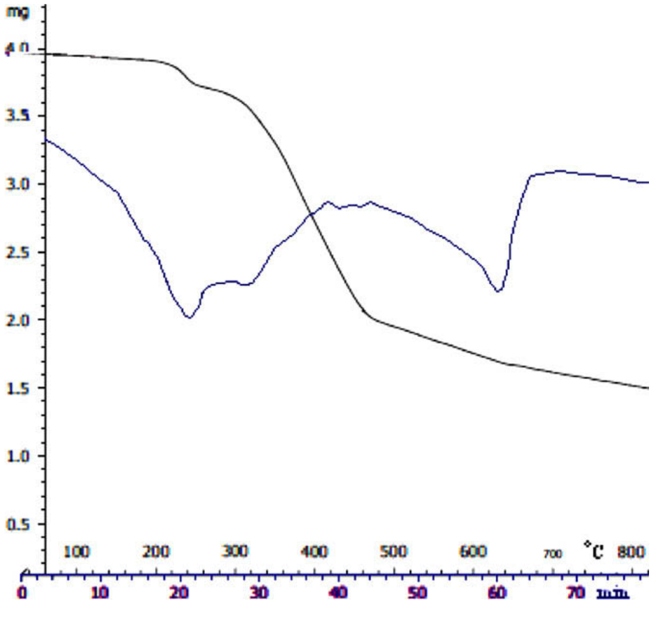

Fig. 2. TG-DTA curve of $[Co(L_1)(H_2O)Cl]$.

3.4. ESR spectra

To obtain further information about the stereochemistry and the site of the metal–ligand bonding and to determine the magnetic interaction in the metal complexes, the X-band ESR spectra of all Cu(II) complexes have been recorded in the polycrystalline state. The ESR spectra of Cu(II) complexes exhibit a single broad signal (Fig. 3) due to dipolar broadening and enhanced spin lattice relaxation. The spectra of all Cu(II) complexes are quite similar and exhibit auxiliary symmetric g-tensor parameters with $g_{||} > g_{\perp} > 2.0023$ indicating that the copper site has a $d_{x^2-y^2}$ ground state characteristic of octahedral geometry [35]. The observed g values for all Cu(II) complexes are less than 2.3 and are in agreement with the covalent character of the metal–ligand bond. No band corresponding to $\Delta Ms = \pm 2$ transition is observed in the spectrum ruling out any Cu–Cu interaction. The geometric parameter G, which is a measure of exchange interaction between the copper centres in the polycrystalline compounds, is calculated using the equation $G = (g_{||} - 2.0023)/(g_{\perp} - 2.0023)$. According to Hathaway [36,37], if the value of G is greater than four, the exchange interaction between Cu(II) centers in the solid state is negligible, whereas when it is less than four, a considerable exchange interaction is indicated in the solid complex. The calculated G values are within the range 3.44–3.83 for all copper complexes indicating that the magnetic interaction between the Cu(II) ions is negligible in the solid complexes [38].

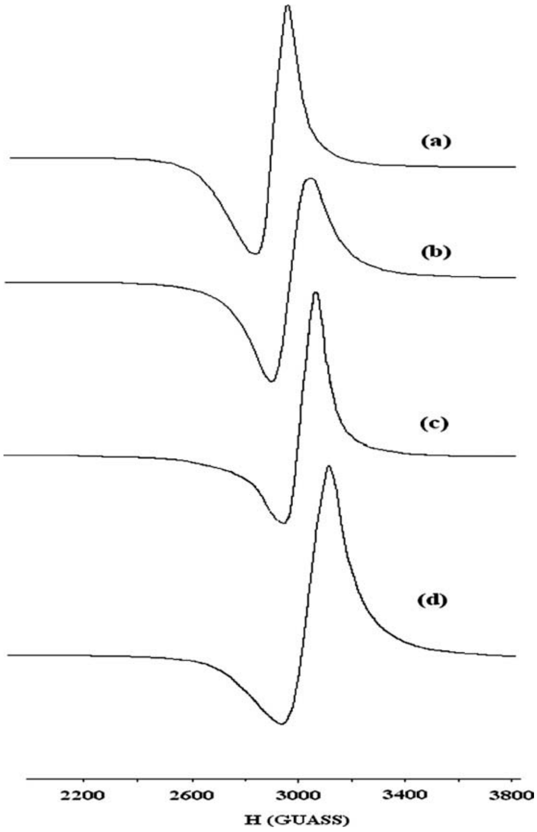

Fig. 3. X-band polycrystalline ESR spectra of the complexes $[Cu(L_1)(H_2O)Cl]$ (a), $[Cu(L_2)(H_2O)Cl]$ (b), $[Cu(L_3)(H_2O)Cl]$ (c), $[Cu(L_4)(H_2O)Cl]$ (d).

Table 4
Electrochemical data for Ni(II) complexes.

Compound	Reduction potentials						Oxidation potentials		
	E_{pa} (V)	E_{pc} (V)	$E_{1/2}$ (V) ΔE_p (mV)	E_{pa} (V)	E_{pc} (V)	$E_{1/2}$ (V) ΔE_p (mV)	E_{pa} (V)	E_{pc} (V)	$E_{1/2}$ (V) ΔE_p (mV)
$[Ni(L_1)(H_2O)Cl]$	−1.30	−1.42	−1.36 (119)	−0.62	−0.75	−0.69 (136)	+0.42	+0.30	+0.36 (124)
$[Ni(L_2)(H_2O)Cl]$	−1.22	−1.34	−1.28 (123)	−0.56	−0.70	−0.62 (140)	+0.39	+0.28	+0.34 (116)
$[Ni(L_3)(H_2O)Cl]$	−1.26	−1.39	−1.33 (131)	−0.57	−0.71	−0.64 (136)	+0.41	+0.28	+0.34 (129)
$[Ni(L_4)(H_2O)Cl]$	−1.18	−1.30	−1.24 (119)	−0.53	−0.67	−0.60 (146)	+0.39	+0.27	+0.33 (115)

Supporting electrolyte: $n\text{-}Bu_4NClO_4$ (0.05 M); complex: 0.001 M; solvent: DMF; $\Delta E_p = E_{pa} - E_{pc}$ where, E_{pa} and E_{pc} are anodic and cathodic potentials, respectively; $E_{1/2} = ½(E_{pa} + E_{pc})$; scan rate:50 mV s^{-1}.

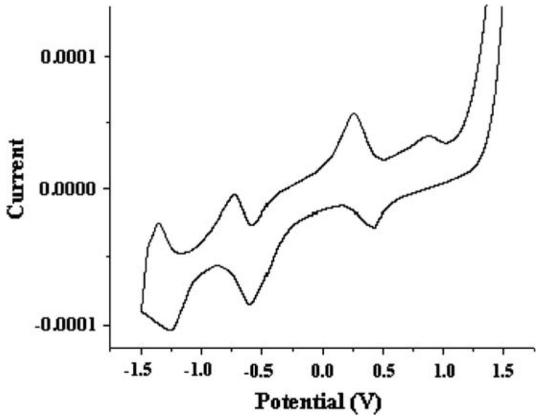

Fig. 4. Cyclic voltammogram of $[Ni(L_3)(H_2O)Cl]$.

Table 5
X-ray diffraction data of $[Ni(L_1)(H_2O)Cl]$.

d (Å)	I/I_0	$\sin^2\theta$ Obs.	$\sin^2\theta$ Calc.	hkl	2θ Obs.	2θ Calc
7.361	10.1	109.5	109.5	110	12.01	12.01
6.592	17.6	136.5	136.5	111	13.42	13.42
6.247	12.8	152.0	162.9	102	14.17	14.67
5.013	21.3	236.1	243.3	003	17.68	17.95
4.820	18.4	255.4	246.0	201	18.39	18.05
4.271	23.1	325.2	327.1	202	20.78	20.84
3.914	12.4	387.3	381.9	212	22.70	22.54
3.386	17.5	517.5	517.1	213	26.30	26.29
3.147	32.9	599.1	600.9	302	28.34	28.38
3.115	100.0	611.4	651.6	204	28.63	29.58
2.826	18.7	742.9	738.8	321	31.63	31.54
2.343	7.6	1080.7	1082.8	116	38.39	38.42
2.073	14.8	1380.6	1379.5	107	43.62	43.61
2.029	17.6	1441.1	1434.3	117	44.62	44.51
1.783	9.3	1866.2	1861.4	530	51.19	51.12

Table 6
X-ray diffraction data of $[Cu(L_1)(H_2O)Cl]$.

d (Å)	I/I_0	$\sin^2\theta$ Obs.	$\sin^2\theta$ Calc.	hkl	2θ Obs.	2θ Calc.
7.823	9.1	96.9	96.9	1 0 1	11.30	11.30
7.312	13.4	111.0	111.0	2 0 0	12.09	12.09
6.491	17.8	140.8	138.72	2 1 0	13.63	13.53
5.712	19.3	181.8	180.2	2 0 1	15.50	15.43
4.861	11.2	251.1	249.7	3 0 0	18.23	18.18
3.987	13.5	373.2	360.6	3 2 0	22.28	21.89
3.468	16.2	493.3	498.7	2 2 2	25.67	25.81
3.095	13.3	619.4	622.8	0 0 3	28.82	28.90
2.762	34.7	777.7	776.2	3 3 2	32.39	32.35
2.134	100.0	1302.8	1303.3	6 1 2	42.32	42.32
2.089	21.9	1359.5	1359.4	7 0 0	43.27	43.27
2.019	9.6	1455.4	1456.3	5 5 1	44.85	44.87
1.737	14.8	1966.4	1969.1	6 5 2	52.65	52.69

3.5. Cyclic voltammetry

The electrochemical properties of all the Ni(II) complexes were investigated in DMF solution (10^{-3} M) containing 0.05 M $n\text{-}Bu_4NClO_4$ as supporting electrolyte by cyclic voltammetry. All the measurements were carried out in the potential range +1.5 to −1.5 V with scan rate 50 mV s^{-1} and redox potentials are expressed with reference to Ag/AgCl. The potentials are summarized in Table 4 and representative voltammogram of $[Ni(L_3)(H_2O)Cl]$ is shown in Fig 4.

The cyclic voltammogram of Ni(II) complexes displayed both anodic and cathodic redox processes. In anodic region the reduction wave (E_{pc}, +0.277 to +0.302 V) corresponding to Ni(III)/Ni(II) process is obtained. During reverse scan the oxidation of Ni(II)/Ni(III) occurs in the potential range (E_{pa}, +0.392 to +0.426 V). The oxidation observed is quasireversible in nature, characterized by a large peak-to-peak separation (ΔE_p) of 115–129 mV. In cathodic potential region, the complexes display two quasireversible redox couples at −0.60 to −0.69 V (ΔE_p, 136–146 mV) and −1.24 to −1.36 V (ΔE_p, 119–131 mV), may be assigned to reduction of the azo group [(-N=N-)/(-N=N-)$^-$] and [(-N=N-)$^-$/(-N=N-)$^{2-}$], respectively, of the chelated ligand.

3.6. X-ray powder diffraction

Single crystal X-ray crystallographic investigation is the most precise source of information regarding the structure of the complexes, but the difficulty of obtaining crystalline complexes in proper symmetric form has rendered the powder X-ray diffraction method for such study. The X-ray diffraction pattern of $[Mn(L_1)(H_2O)Cl]$ and $[Co(L_1)(H_2O)Cl]$ complexes are similar in nature having no peaks. The trend of the curves decreases from maximum to minimum intensity indicating that these complexes are amorphous in nature in the present metal–ligand formation. The X-ray diffraction pattern of $[Ni(L_1)(H_2O)Cl]$ and $[Cu(L_1)(H_2O)Cl]$ indicates high crystallinity of the complexes. The diffractogram of $[Ni(L_1)(H_2O)Cl]$ records 15 reflections between 5° and 80° (2θ) with maximum at 2θ = 28.63° corresponding to value of d = 3.115 Å (Table 5). However, the diffractogram of $[Cu(L_1)(H_2O)Cl]$ consists of 13 reflections with maxima at 2θ = 42.32° corresponding to value of d = 2.134 Å (Table 6). The main peaks of $[Ni(L_1)(H_2O)Cl]$ and $[Cu(L_1)(H_2O)Cl]$ have been indexed by using computer software by trial and error method, keeping in mind characteristics of various symmetry systems until good fit could be obtain between observed and calculated 2θ and $\sin^2\theta$ values. The method also yielded *hkl* (Miller indices) values. The relative intensities corresponding to prominent peaks have also been measured.

The indexing of diffractogram of $[Ni(L_1)(H_2O)Cl]$ and $[Cu(L_1)(H_2O)Cl]$ are identical. Based on this it can be proposed that these compounds belong to same structural class. A comparison of the values of 2θ and $\sin^2\theta$ for the $[Ni(L_1)(H_2O)Cl]$ and $[Cu(L_1)(H_2O)Cl]$ complexes reveals that, there is good agreement between the calculated and observed value of 2θ and $\sin^2\theta$ on the basis of assumption of tetragonal structure [39]. The small difference in the observed *d* spacing can be attributed to difference in unit cell dimensions. The structure of $[Ni(L_1)(H_2O)Cl]$ yields values for lattice constant $a = b = 10.410$ Å, $c = 14.810$ Å and unit cell volume $V = 1605.32$ Å^3. However the structure of $[Cu(L_1)(H_2O)Cl]$ yields values for lattice constant $a = b = 14.624$ Å, $c = 9.259$ Å and unit cell volume $V = 1980.19$ Å^3. In conjugation with these lattice parameters the condition [40,41] such as $a = b \neq c$ and of $\alpha = \beta = \gamma = 90^\circ$ required for the samples to be tetragonal were tested and found to be satisfactory.

4. Conclusions

On the basis of physico-chemical characterization, the ligands HL_{1-4} behave as monobasic and coordinate to the metal ions in tetradentate manner with NNNS donor sites. Magnetic moment and electronic spectra indicates octahedral geometry for Mn(II), Co(II) and Ni(II) complexes and distorted octahedral geometry for the Cu(II) complexes. The ESR spectra of Cu(II) complexes were studied resulting into $g_{||} > g_{\perp} > 2.0023$ suggesting that the metal–ligand bonds have considerable covalent character. Electrochemical studies of the complexes show quasireversible Ni(III)/Ni(II) couple along with ligand reduction. The X-ray diffraction studies indicate that the Mn(II) and Co(II) complexes are amorphous in nature in the studied metal–ligand formation. However, Ni(II) and Cu(II) complexes are polycrystalline in nature showing tetragonal crystal structure.

Acknowledgement

The authors express their sincere thanks to University Grants Commission, New Delhi for financial assistance.

References

[1] S. Patai, The Chemistry of the Hydrazo, Azo and Azoxy Groups, Part 1, Wiley, New York, 1975.
[2] Z.W. Myslak, M.M. Bolt, Prophyl. Ergon. 38 (1988) 310.
[3] A.I. Vogel, A Textbook of Quantitative Analysis, fourth ed., ELBS and Longman, London, 1978.
[4] R. Kilincarslan, E. Erdem, Trans. Met. Chem. 32 (2007) 102.
[5] A.G. Makhsumov, M.S. Ergashev, F.A. Normatov, Pharm. Chem. J. 25 (1991) 1.
[6] I.M. Awad, A.A. Aly, A.M. Abdel Alim, R.A. Abdel Aal, S.H. Ahmed, J. Inorg. Biochem. 33 (1998) 77.
[7] A.A. Jarahpour, M. Motamedifar, K. Pakshir, N. Hadi, Z. Zarei, Molecules 9 (2004) 815.
[8] M. Huang, S. Wu, J. Wang, C. Lin, S. Lu, L. Liao, A. Shen, Drug Dev. Res. 60 (2003) 261.
[9] S. Samadhiya, H. Halve, Orient. J. Chem. 17 (2001) 119.
[10] W.M. Fabian, L. Antony, D. Nedeltcheva, F.S. Kamounad, P.J. Taylor, J. Phys. Chem. 108 (1997) 7603.
[11] X. Chen, J. Zhang, H. Zhang, Z. Jiang, G. Shi, Y. Li, Y. Song, Dyes Pigments 77 (2008) 223.
[12] H. Wada, T. Ishizuki, G. Nakagawa, Anal. Chim. Acta 135 (1982) 333.
[13] X. Fan, C. Zhu, Mikrochim. Acta 126 (1997) 59.
[14] V.A. Lemos, E.S. Santos, M.S. Santos, R.T. Yamaki, Microchim. Acta 158 (2007) 189.
[15] S. Wu, W. Qian, Z. Xia, Y. Zou, S. Wang, S. Shen, H. Xu, Chem. Phys. Lett. 330 (2000) 535.
[16] Z.M. Zaki, Spectrochim. Acta A 56 (2000) 917.
[17] P.P. Hankare, S.S. Chavan, Synth. React. Inorg. Met.-Org. Chem. 33 (3) (2003) 423.
[18] M.M. Omar, G.G. Mohamed, Spectrochim. Acta A 61 (2005) 929.
[19] B. Dash, M.K. Rout, J. Ind. Chem. Soc. 32 (1955) 663.
[20] P.B. Talukdar, S.K. Sengupta, A.K. Datta, T.K. Roy, Indian J. Chem. 15B (1977) 41.
[21] A.S. El-Azab, Phosphorous Sulfur Silicon 182 (2007) 333.
[22] H.H. Hovind, Analyst Rev. 100 (1975) 769.
[23] B. Singh, M.M.P. Rukhaiyar, R.J. Sinha, J. Inorg. Nucl. Chem. 39 (1977) 29.
[24] K. Krishnankutty, D.K. Babu, J. Indian Chem. Soc. 73 (1996) 379.
[25] S.S. Kandil, G.B. El-Hefnawy, E.A. Bakr, A.Z. Abou El-Ezz, Trans. Met. Chem. 28 (2003) 168.
[26] P.F. Raphel, E. Manoj, M.R. Prathapachandra Kurup, Polyhedron 26 (2007) 818.
[27] B.K. Singh, P. Mishra, B.S. Garg, Trans. Met. Chem. 32 (2007) 603.
[28] P.P. Birnbaum, J.H. Linford, D.W.G. Style, Trans. Faraday Soc. 49 (1953) 735.
[29] V.P. Daniel, B. Murukan, B. Sindhu Kumari, K. Mohanan, Spectrochim. Acta A 70 (2008) 403.
[30] M. El-Behery, H. El-Twigry, Spectrochim. Acta A 66 (2007) 26.
[31] Z.H. Abd El-Waheb, Spectrochim. Acta A 67 (2007) 25.
[32] S. Chandra, M. Pundir, Spectrochim. Acta A 69 (2008) 1.
[33] N.V. Thakkar, S.Z. Bootwala, Synth. React. Inorg. Met.-Org. Chem. 26 (1996) 1053.
[34] I. Yilmaz, H. Temel, H. Alp, Polyhedron 27 (2008) 125.
[35] G. Speir, J. Csihony, A.M. Whalen, C.G. Pierpont, Inorg. Chem. 35 (1996) 3519.
[36] B.J. Hathaway, D.E. Billing, Coord. Chem. Rev. 5 (1970) 143.
[37] B.J. Hathaway, Struct. Bond. 57 (1984) 55.
[38] S.A. Sallam, Trans. Met. Chem. 31 (2006) 46.
[39] P.P. Hankare, S.S. Chavan, Indian J. Chem. 42A (2003) 456.
[40] H.P. Klug, L.E. Alexander, X-ray diffraction procedure for polycrystalline and amorphous material, John Wiley and sons, Inc., NY, London, 1974.
[41] B.D. Cullity, Elements of X-Ray Diffraction, second ed., Addison-Wesley, 1977.